

Surface Viscoelastic Parameters of Poly((dimethylamino)ethyl methacrylate–methyl methacrylate) Diblock Copolymer Solutions: pH Dependence of the Evolution of the Equilibrium Values

Andrew J. Milling and Randal W. Richards*

IRC in Polymer Science and Technology, University of Durham, Durham DH1 3LE, UK

Fiona L. Baines, Steven P. Armes, and Norman C. Billingham

School of Chemistry, Physics and Environmental Sciences, University of Sussex, Brighton BN1 9QJ, UK

Received September 26, 2000; Revised Manuscript Received February 22, 2001

ABSTRACT: The dynamic interfacial properties of a diblock copolymer poly((dimethylamino)ethyl methacrylate-*b*-methyl methacrylate) have been obtained by surface quasi-elastic light scattering. The temporal evolution of the capillary wave frequency and damping as well as the surface viscoelastic properties (surface tension, dilational modulus, and dilational viscosity) of a freshly formed air–water interface for a range of pH values (at fixed scattering vector) has been investigated. The equilibration dynamics were dependent on the solution pH, but the equilibrium state was obtained by the time the interface was 12 h old. Tensiometry showed that a surface phase transition occurs between pH 7.0 and pH 6.0. The surface light scattering data clearly showed the differences in temporal response in this same range of pH. For solutions with pH 5.0, the air–water interface is populated by unimers. For higher pH solutions, micelles are the initial species at the surface, but these disaggregate for solutions with pH 6.0 and 6.5. The disaggregation process is faster for the solution with pH 6.5, and this is associated with resonance between the capillary and dilational modes enabling energy to be transferred to the dilational mode, accelerating the disaggregation of the micelles.

Introduction

The adsorption of block copolymers at interfaces is of interest for both academic study and technological applications. In solution, block copolymers can display a wide range of structural behavior, depending upon the solvency conditions and the molecular architecture. In many cases preferential solvation of one block bestows surface activity and self-aggregation to micelles and eventually organization with considerable long-range order. At low concentrations, solution structures of partially soluble copolymers are generally confined to unimers and micelles; the micellar states themselves may be of various geometries depending on copolymer composition and solution concentration. The majority of block copolymers studied have electrically neutral blocks; a relatively novel class of block copolymers composed of an electrically neutral block and a polyelectrolyte block have been explored of late. The aqueous solution behavior of these copolymers is dependent upon the ionic strength and, for weak polyelectrolytes, the solution pH. The linear diblock copolymer poly((dimethylamino)ethyl methacrylate-*b*-methyl methacrylate) (poly(DMAEMA-*b*-MMA)) is one such a copolymer, and its organization in both aqueous solution at the interface of the aqueous solution with air and a solid¹ has been explored by others using dynamic light scattering, neutron reflectometry, and ellipsometry. However, the role of these polymers in modifying surface fluctuations (capillary waves) and associated interfacial surface viscoelastic moduli has not been reported. Surface quasi-elastic light scattering (SQELS) is a nonperturbative method for the investigation of capil-

lary wave phenomena that has been applied to pure liquid interfaces, surfactant and polymer excess layers (Gibbs films), and spread polymer films (Langmuir films) at fluid interfaces. For adsorption from solution, the dynamics of adsorption and relaxation may be slow, and hence the rapid data acquisition times of SQELS experiments allow “snapshots” of the interface to be made over time during surface reorganization and surface-bulk equilibration. Consequently, insight into the mechanism of interfacial structure formation may be gained.

We report here the findings of SQELS experiments performed on aqueous solutions of poly(DMAEMA-*b*-MMA) at fixed concentration but over a range of pH. First, the theoretical background to the SQELS experiment and the extraction of pertinent information is outlined. The details of the light scattering and tensiometric experiments are given before concluding with a discussion of the results and a comparison with the surface organization data from the earlier neutron reflectometry experiments on similar copolymers.

Theoretical Background

The surfaces of liquids are continually roughened by thermal fluctuations that can be decomposed into a discrete set of Fourier modes, the capillary waves.² The relationship between the frequency and wavenumber (q) of these Fourier modes is described by a dispersion equation.^{3,4} For a pure liquid surface the dispersion equation is couched in terms of the surface tension (γ_0), the bulk density (ρ), and viscosity (η).⁵ The complex frequency of the capillary wave, ω ,

$$\omega = \omega_0 + i\Gamma \quad (1)$$

* To whom correspondence should be addressed.

has a real frequency (ω_0) and a damping term (Γ). For a pure liquid, the roots of the dispersion equation, i.e., ω_0 and Γ , are approximately given by eqs 2 and 3.

$$\omega_0 = \left(\frac{\gamma_0 q^3}{\rho} \right)^{1/2} \quad (2)$$

$$\Gamma = \frac{2\eta q^2}{\rho} \quad (3)$$

where q is the surface wavenumber observed.

Lucassen^{3,6} showed that when a second species was present as either a spread film or a surface excess, dilational (longitudinal) modes exist at an air–water interface in addition to the capillary (transverse) modes. Goodrich^{7,8} discussed these and a further three surface dynamic modes from a theoretical viewpoint, the additional modes being lateral shear, horizontal shear, and vertical compression. Only the capillary and dilational modes are of interest here since it is only these that influence the dispersion equation for light scattered from the fluctuating surface.

Recently, Buzza et al.⁹ reexamined the dispersion equation pertinent to polymer layers at fluid interfaces, and a new form was obtained that includes a term quantifying the bending mode of an interfacial film and an asymmetry term describing an additional source of coupling between the dilational and capillary modes. In this case the dispersion equation is given by

$$D(\omega) = [\eta\omega(q - m) + i\tilde{\epsilon}q^2]^2 + [\tilde{\epsilon}q^2 + i\eta\omega(q + m)][(\gamma + \tilde{\kappa}q^2)q^2 + i\eta\omega(q + m) - \rho\omega^2/q] \quad (4)$$

where

$$m = (q^2 + i\omega\rho/\eta)^{1/2} \quad (5)$$

(for $\text{Re}(m) > 0$), and the three complex viscoelastic parameters are

$$\tilde{\epsilon} = \epsilon_0 + i\omega\epsilon' \quad (6)$$

$$\tilde{\kappa} = \kappa_0 + i\omega\kappa' \quad (7)$$

$$\tilde{\lambda} = \lambda_0 + i\omega\lambda' \quad (8)$$

where ϵ_0 , κ_0 , and λ_0 are the dilational, bending, and coupling moduli, respectively, and the primed terms are viscosity terms incorporated from linear response theory to account for any dissipative processes. In principle, an equation for the complex surface tension, $\tilde{\gamma}$, similar in form to eq 6 can be written down; however, the transverse shear viscosity, γ' , has been shown to be nonexistent.⁹

The capillary mode is by far the predominant source of surface scattered light. Energy transfer between photons and capillary waves on scattering leads to a broadening of the power spectrum of the scattered light. Because the power spectrum (eq 9)

$$P_{\text{CAP}}(\omega) = \frac{2k_B T}{\omega} \text{Im} \left[\frac{\tilde{\epsilon}q^2 + i\eta\omega(q + m)}{D(q, \omega)} \right] \quad (9)$$

incorporates the dispersion equation, then the surface viscoelastic moduli influence its shape. The influence of the dilational modes is indirect, since their contribution is only observed as a result of the coupling between

capillary and dilational modes; nonetheless, their effect on surface wave frequency and damping can be profound.

Experimental Section

Materials. The poly(DMAEMA-*b*-MMA) diblock copolymer had a mole fraction of DMAEMA units of 0.8 and a total number-average molecular weight of 42 000 g mol⁻¹ with a polydispersity of 1.15. The synthesis of this and similar block copolymers has been discussed previously.¹⁰ All water used was purified to electrochemical purity levels, i.e., a resistance of 18 Mohm, and analytical grade methanol was used as received.

Stock solutions were prepared by dissolving the polymer in methanol followed by filtering through a 0.1 μm filter (Millipore type VVLP). This solution was then further diluted with methanol and water to a final mixed solvent composition of 5% (w/v) methanol and a polymer content of 0.1% (w/v). The pH of each solution was adjusted by addition of small aliquots of hydrochloric acid (BDH, AnalaR grade); the discrete pH values investigated were 5.0, 6.0, 6.5, 7.0, and 7.5. Solutions were stored in sealed volumetric flasks to exclude ambient carbon dioxide for 24 h prior to use, during which time the pH remained stable.

Surface Quasi-Elastic Light Scattering (SQELS). A heterodyne technique is necessary to separate the scattering due to the capillary waves from the incident light frequency because the frequency shift of the scattered light is small. The optical train used has been described many times before, and the temporal evolution of the scattered light (i.e., the correlation function) was observed rather than the frequency distribution of the power spectrum. Repeated data collections over several hours, while the surface was approaching equilibrium, were made using a Brookhaven BI900 digital correlator. When the air–water interface had reached equilibrium, SQELS data were collected for a range of scattering vector, q , using a Brookhaven BI2030 digital correlator. In both cases the correlator delay channels were linearly spaced. The design of the trough used did not allow an inert atmosphere to be maintained above the interface; consequently, for aqueous phases with initial pH > 7.5, slow adsorption of CO₂ reduced the bulk pH. This effect notwithstanding, buffering of the bulk solution by the weakly basic amine residues of the copolymer ensures the pH does not fall below 7.5 even with CO₂ adsorption. For solutions with an initial pH \leq 7.5, the value remained constant with time, and thus our SQELS experiments were confined to solutions whose pH did not exceed 7.5.

The correlation functions obtained were analyzed in two ways: first, the frequency and damping were obtained using an objective cosine fit;^{11,12} second, the surface viscoelastic parameters (γ_0 , ϵ_0 , and ϵ') were obtained by the direct analysis developed by Earnshaw.¹³ In both cases factors for the instrumental broadening, low-frequency building vibrations, photomultiplier tube “ringing”, etc., were incorporated. The adjustables in the fitting procedure to obtain the surface viscoelastic moduli were the surface tension, dilational modulus, and dilational viscosity; the transverse shear viscosity was set to zero as outlined earlier. For the conditions of the experiments reported here, i.e., maximal coupling between dilational and capillary modes, a thin polymer layer, and a large interfacial tension, the bending and the asymmetry contributions of eqs 7 and 8 are also negligible.^{3,9} A typical correlation function and the fit of the dispersion equation to the data are shown in Figure 1.

Tensiometry. Tensiometry measurements on the polyDMAEMA-*b*-MMA solutions were performed using a Krüss K10 tensiometer and a Du Nouy ring. Each solution/air interface was allowed to age (under a Parafilm seal) for up to 24 h prior to measurement. Because of surface disruption repeat measurements were not possible for a single solution, however, repeated measurements using fresh solutions were reproducible to within ± 0.25 mN m⁻¹.

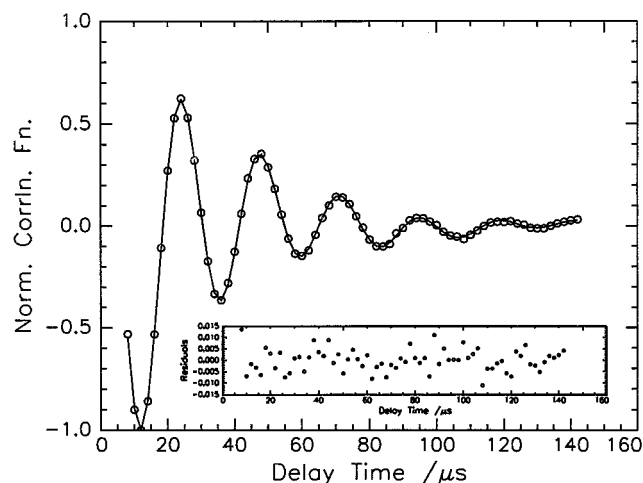


Figure 1. A typical correlation curve obtained at pH 6.0, $q = 1035 \text{ cm}^{-1}$, and $T = 298 \text{ K}$. The line through the data points is the fit from the spectral fitting method. The inset shows the fitting residuals.

Results

We present the results in two broad sections: the variation with time after formation of the fresh surface and the equilibrium values of the capillary wave parameters. Within each of those broad classifications first the frequency and damping dependence on the pH of the solution are compared, followed by the surface viscoelastic moduli.

Time Dependence of the Air–Solution Interface.

Capillary Wave Frequency and Damping. For these experiments, the wave vector was fixed at $q = 1035 \text{ cm}^{-1}$, sufficiently remote from the q range where oscillatory photomultiplier tube effects would interfere but not so high that overdamping of the capillary and dilational modes would produce atypical results. Since frequency and damping of the capillary waves are q -dependent and this in its turn has a strong dependence on the liquid surface height, it was important to verify that evaporation losses did not occur with time that could be interpreted as a change in interfacial properties due to other factors. A control experiment on the mixed solvent alone showed less than 0.5% variation in capillary wave frequency and damping over a period of 12 h. For a temperature of 298 K, these values were $\omega_0 = 260.7 \pm 0.5 \text{ kHz}$ and $\Gamma = 21.3 \pm 0.1 \text{ kHz}$. Consequently, evaporation of the solvent mixture is negligible and has no influence on the interpretation of the results. The evolution with time of the capillary wave frequency with age of the solution surface for each pH investigated is shown in Figures 2 and 3.

For solutions with pH 7.5, 7.0, and 6.0 capillary wave frequencies (Figure 2) increase with time, the rate of increase becoming faster as pH decreases. Approximately constant values are reached after 6 h, these constant values increasing for lower pH values. The frequency for the pH 5.0 solution is constant with age of the surface, and the asymptotic values of the time dependences of the higher pH solutions noted above approach this constant value. For the solution with pH 6.5 the frequency variation with time is quite different (Figure 3a), a rapid increase in frequency is evident, the asymptotic value being reached after $\sim 3.5 \text{ h}$, and this asymptotic value is identical with the constant frequency of the pH 5.0 solution. Figure 4 shows the damping for the majority of the solutions; for pH 7.0

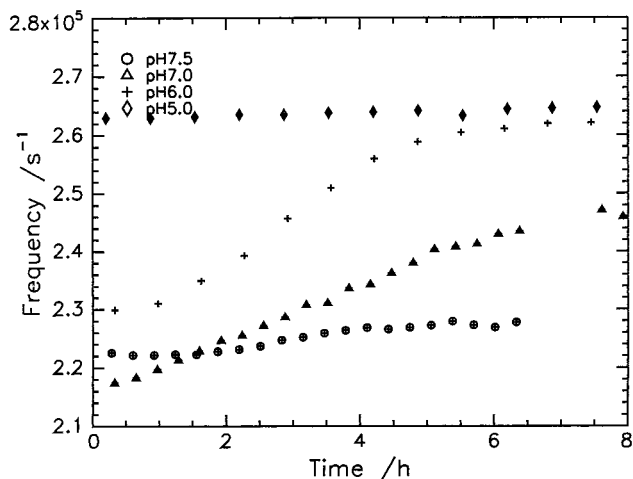


Figure 2. Capillary wave frequency at $q = 1035 \text{ cm}^{-1}$ and a temperature of 298 K for a 0.1% (w/v) poly(DMAEMA-*b*-MMA) as a function of time for solutions of pH 7.5, 7.0, 6.0, and 5.0.

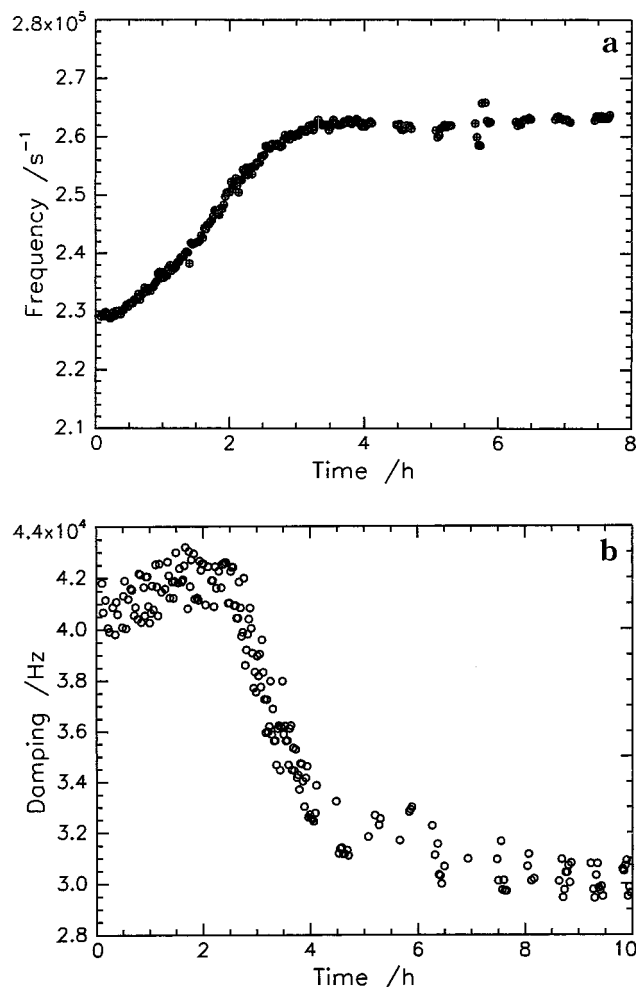


Figure 3. Time dependence of the capillary wave frequency (a) and damping (b) for poly(DMAEMA-*b*-MMA) solution with pH 6.5. All other conditions as in Figure 2.

and 7.5 the damping increases with time from a low value to an asymptotic value after ca. 6 h. However, the pH 6.0 solution exhibits very different behavior, starting at a high damping and falling after 4 h to a value approaching the low constant damping of the pH 5.0 solution. This same type of behavior, but in a much more marked form, was exhibited by the pH 6.5 solution (Figure 3b). For this solution the damping has a slight

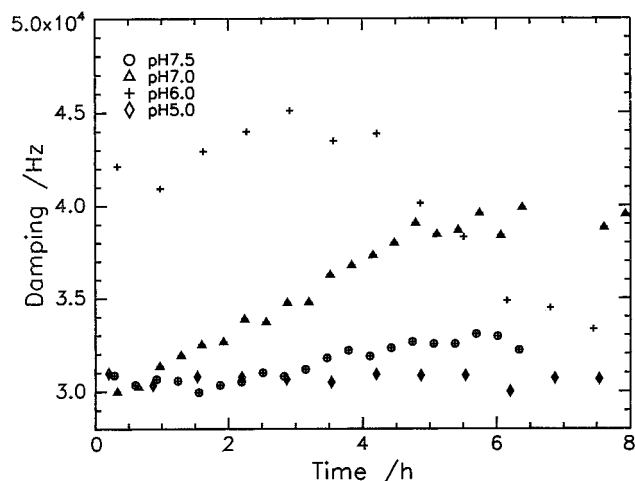


Figure 4. Capillary wave damping for all poly(DMAEMA-*b*-MMA) solutions as a function of time under the conditions given for Figure 2.

increase for the first 2 h and then falls at a roughly constant rate over the next 2 h to a lower constant damping that is slightly larger than the value for the pH 5.0 solution.

Surface Viscoelastic Parameters. Figure 5 shows the dependence of the surface viscoelastic parameters on the age of the air–solution interface for all the pH values investigated. Apart from pH 5.0, the surface tensions of all the solutions rise with time to a plateau value, the plateau value increasing with decrease in the pH of the solutions. For the pH 5.0 solution there is no dependence on the age of the interface, the surface tension being approximately constant at 64.5 mN m^{-1} . This latter value is that eventually attained by the solution of pH 6.5 and is approached at a much faster rate than in solutions of higher pH. The dilational modulus for the pH 5.0 solution remains constant at the low value of 9.5 mN m^{-1} , the value eventually reached by the pH 6.0 and 6.5 solutions after starting at higher values of ca. 12.5 mN m^{-1} . This value is reached after a much shorter time for the pH 6.5 solution than that for pH 6.0; additionally, after ca. 4 h there is evidence for an additional factors contributing to the dilational modulus for the pH 6.5 solution. This is seen as a sharp increase in the dilational modulus before the values fall again to ca. 9.5 mN m^{-1} . For the solutions with pH 7.0 and 7.5 the final dilational moduli are higher values than that for the solutions of lower pH. The most remarkable changes are seen in the dilational viscosities. Again, the pH 5.0 solution has a constant value at $1.1 \times 10^{-5} \text{ mN m s}^{-1}$; pH 7.0 and 7.5 solutions start at this value but then fall to low constant values. In the case of pH 7.0 the final value is negative. Very different behavior is displayed by the pH 6.0 and pH 6.5 solutions. In the case of the former, the initial value is small and negative and then falls to a minimum after 2 h followed by a steady increase to a value of $0.5 \times 10^{-5} \text{ mN m s}^{-1}$ after 7 h. The early time behavior of the pH 6.5 solution follows that for pH 6.0, but a sharp increase takes place after 2 h to the dilational viscosity of the pH 5.0 solution.

pH Dependence of Equilibrium Values. Figure 6 shows the dependence on pH of the various surface viscoelastic parameters and the static surface tensions after the surface has aged 24 h. The capillary wave frequency is constant from pH 5 to pH 6.5 whereupon

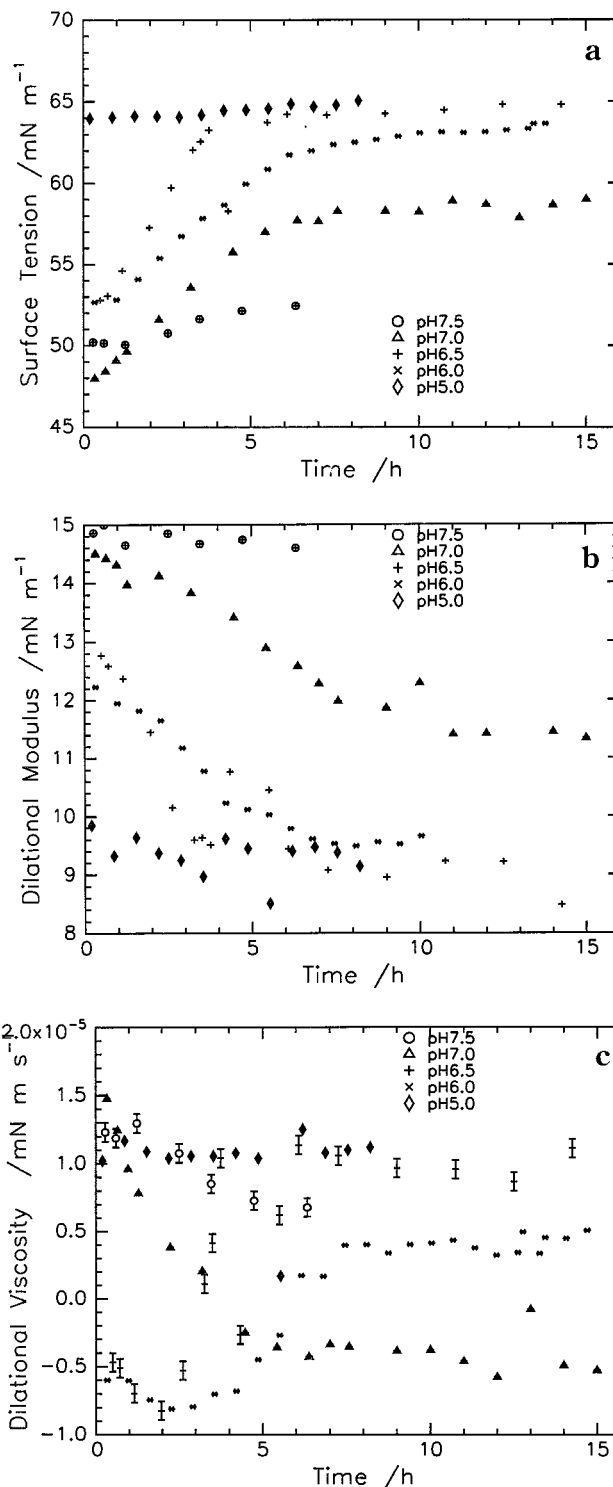


Figure 5. Dependence of surface viscoelastic parameters on age of air–water interface: (a) surface tension; (b) dilational modulus; (c) dilational viscosity.

it falls continuously as the pH increases. This phenomenology is reflected somewhat in the surface tension values extracted from the light scattering data, but a rather richer behavior is evident that parallels the zero frequency values of surface tension obtained by tensiometry. For these latter data the surface tension falls continuously from pH 5 to pH 6; thereafter, it increases until pH 7 is reached when it falls again with further increase in pH. The SQELS values of surface tension follow this behavior but with higher values of surface tension (reflecting the frequency dependence of surface

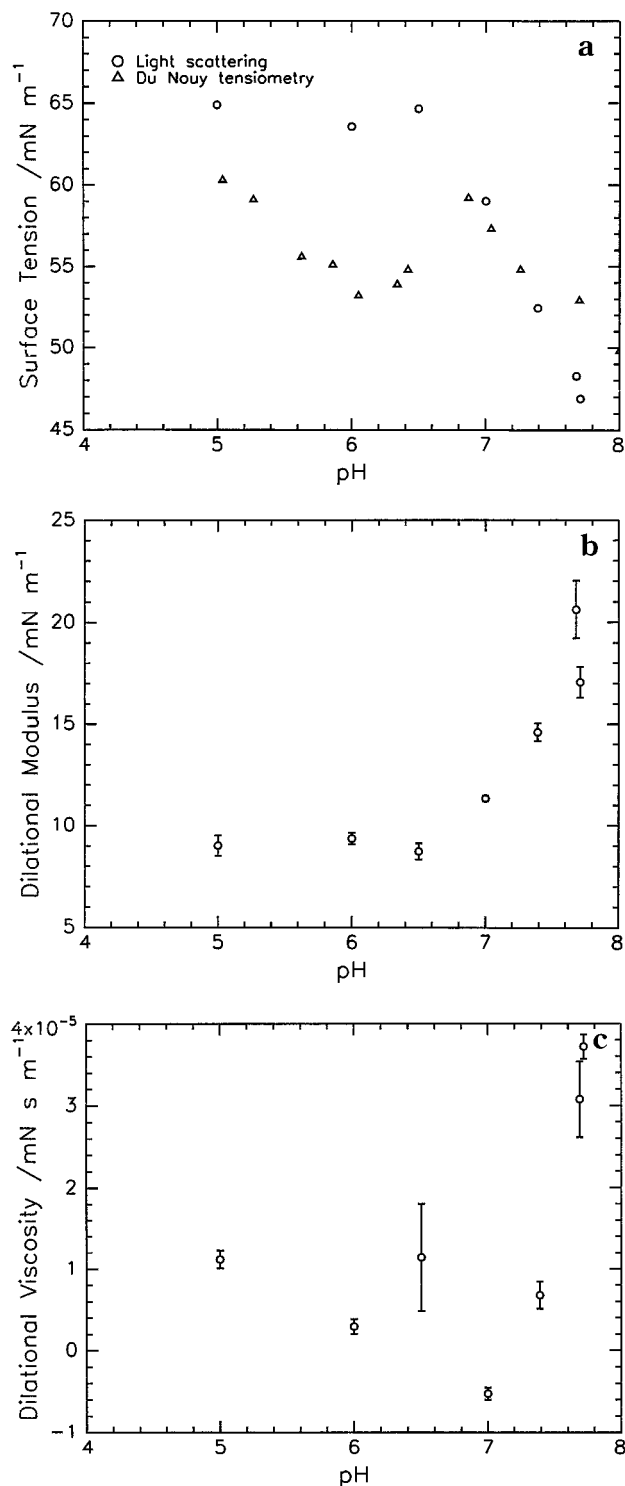


Figure 6. Equilibrium surface viscoelastic parameters as a function of pH at $q = 1035 \text{ cm}^{-1}$ and a temperature of 298 K: (a) surface tension (from SQELS and tensiometry); (b) dilational modulus; (c) dilational viscosity.

tension) for pH less than 7. Dilational moduli have a relatively low value of $\sim 9 \text{ mN m}^{-1}$ until pH 6.5 is reached whereupon the value increases rapidly to $\sim 21 \text{ mN m}^{-1}$ at pH 7. Dilational viscosities are much more scattered but are approximately constant at $\sim 5 \times 10^{-6} \text{ mN m s}^{-1}$ for much of the pH range.

Discussion

It is pertinent to review, briefly, the properties of polyelectrolyte containing block copolymers in solution.

Analogous to the behavior of neutral block copolymers in solution, polyelectrolyte containing block copolymers molecules can form a variety of assembled structures. A number of factors determine the nature of the aggregates formed, e.g., relative block sizes, polymer concentration, degree of ionization, and the ionic strength of the aqueous phase in which such copolymers are usually dissolved. For the block copolymers at issue here, the DMAEMA units have weakly basic tertiary amine groups, and thus the extent of ionization and solution properties are strongly effected by pH. In particular, the pK_a for the copolymer of the same composition at the air–water interface has been reported to be 6.8.¹⁴ No salt has been added to the solutions investigated here, and thus they are well within the Debye–Hückel regime of low electrostatic screening. At high pH (>7.5) PCS experiments indicated the uncharged polymers mainly exist as a bimodal mixture of unimers (diameter = $6 \pm 2 \text{ nm}$) and micellar aggregates (diameter = $28 \pm 5 \text{ nm}$). The size of the unimer species is in accordance with a (calculated) 2.5 nm diameter solid PMMA core wrapped in a solvated DMAEMA corona. The size of the micellar species and the marginal solvency of the DMAEMA block suggest that the classical radial-tail spherical micelle structure is unlikely, and an aggregated cluster morphology is conjectured. Reducing the pH increases the extent of ionization of the DMAEMA block, and the solubility of this block increases. At maximum ionization of the DMAEMA block (achieved at ca. 2–3 pH units below the pK_a), the predominant solution species appears to be unimers. In contrast to low molecular weight surfactant behavior, where above the cmc only one species (micelles) dominates, there is a distribution of aggregates and unimers of poly(DMAEMA-*b*-MMA). For $5.0 \leq \text{pH} \leq 7.0$ the wide range of aggregation number entails that the transition from micellar to discrete solution behavior will occur over a finite pH range.

The micellization behavior and surface organization of rather similar copolymers, in terms of composition but of lower total molecular weight, have been reported in earlier publications.^{14–18} For solutions in $\sim 5\%$ methanol in water, the cmc was found to increase as the length of the hydrophobic block (PMMA) or the overall molecular weight of the block copolymer increases.¹⁷ Neutron reflectometry showed that, for 0.1% (w/v) solutions, the surface excess of block copolymer and its layer thickness increased with pH in the manner shown in Figure 7 where the earlier data of An et al.¹⁵ are plotted. The detailed interfacial surface organization was only reported for the two concentrations of 0.04% (w/v) and 0.2% (w/v) at pH values of 6.5, 7.5, and 8.5. At the lowest concentration the surface excess layer is uniform in composition, a more layered structure becoming evident at the higher concentration but with the more soluble DMAEMA block forming the majority of the upper layer which contains no water and appears to be in the air phase. This organization can be rationalized by noting that the surface tension of homopolymeric DMAEMA is lower than that of poly(methyl methacrylate),¹⁹ both being very much lower than that of water. It was suggested that these composition distributions are symptomatic of adsorbed micelles. At high pH (>8) the copolymer is only just soluble because of the low degree of ionization of the DMAEMA block, and the copolymer is highly surface active. At pH 6.5 the DMAEMA block

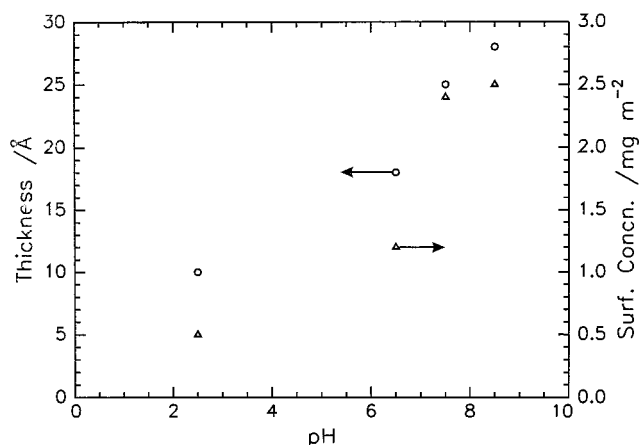


Figure 7. Surface layer thickness and concentration as a function of pH for 0.1% (w/v) solutions of poly(DMAEMA-*b*-MMA). Data obtained from reference 15.

has a much higher degree of ionization (~ 0.63), and the increased charge on the DMAEMA block makes the copolymer more soluble.

However, the dependence of surface tension (and therefore surface coverage by the block copolymer) on pH is rather more complex than suggested in this earlier paper as Figure 6a shows. As the pH increases from 5 to 6, the surface tension decreases commensurate with decreased solubility and increased surface activity. Between pH 6 and 7 there is an increase in surface tension with increasing pH, suggesting a desorption of copolymer or a reorganization of the copolymer at the air–water interface. It is the kinetics of this reorganization that is being followed by the SQELS data of Figures 1–5. Such long times for the surface to reach equilibrium have been seen before in polymeric micellar systems; however, in that case there was a *reduction* of the surface tension over time, indicating a slow population of the surface by micelles that neutron reflectometry data had shown to be present even at bulk concentrations below the cmc. For the poly(DMAEMA-*b*-MMA) copolymer there is an initial rapid absorption at the air–water interface, probably due to the intrinsic negative charge of the water surface, followed by a slow relaxation to the equilibrium organization. We have already noted that the molecular weight of the copolymer used here was considerably larger than that for which the neutron reflectometry data have been reported; thus, some of the observations may be due to this difference in molecular weight.

At the lowest pH of 5.0, the copolymer is adsorbed at the interface as unimers because the degree of ionization of the DMAEMA block is high, promoting molecular solubility rather than micelle formation, and the surface activity is commensurately low. For pH values greater than 6.0, the initial adsorption at the surface appears to be as micelles, but for pH values of 6 and 6.5, these disaggregate with time, desorbing from the interface and a slow increase of surface tension is observed. For pH values of 7 and 7.5, the insolubility and surface activity combine to reduce the extent of disaggregation, and the interfacial layer is composed of a mixture of unimers and micelles, the latter being predominant at the highest pH investigated by SQELS here. The values of the dilational modulus (Figure 5b) also concur with this rationalization. At low pH (5.0) the unimers at the surface contribute little to the in-plane “stiffness” and the dilational modulus is low. At high pH, we now have

micelles at the surface in some form of well-packed array; the corona of the micelle has a brushlike nature.^{20,21} Consequently, the excluded-volume repulsions between brush layers on different micelles would lead to a large dilational modulus as is observed. We note that at pH 7.5 there is no observable time dependence of the dilational modulus. The most significant evidence in favor of the description above is the time dependence of the dilational viscosity. Although the dilational modulus at pH 5 is low, the dilational viscosity is large and positive; this can be attributed to electroviscous effects associated with the high degree of ionization of the DMAEMA block at this pH and the absence of any added salt. At pH 7, the initially high dilational viscosity falls to a *negative* value, indicating that any ionized species initially present rapidly revert to neutral as surface micellization becomes complete. (The notion of negative surface dilational viscosities is discussed further below.) For pH 6 and 6.5 the initial values of the dilational viscosity are negative, suggesting micelles at the surface, but subsequently become positive and approach the dilational viscosity of the pH 5.0 solution, suggestive of disaggregation and ionization. This process seems to be completed when pH = 6.5 in ca. 4 h, but much longer times are needed for solution of pH 6.

The behavior in the region $6.0 \leq \text{pH} \leq 7.0$ is perplexing for the dynamic (SQELS determined) values of the surface moduli. In particular, we note that for pH 6.5 the approach to the equilibrium surface properties is much more rapid than that for pH 6.0 solutions. This appears to contradict the findings of neutron reflectometry¹⁴ and the general trend of surface tension values given above; i.e., as the pH increases, we expect a higher surface coverage by micellar species. Other factors appear to be at work. Observation of dilational properties of capillary waves via light scattering is due to the coupling that exists between the two modes. Because of this coupling and the different dependences of capillary and dilational wave frequencies on the surface tension and dilational modulus, respectively, resonance conditions may occur; i.e., the two frequencies become equal, and there is maximum coupling between the two modes.^{2,22–24} Classically, the condition that needs to be satisfied for resonance between the dilational and capillary modes is that the ratio $\epsilon_0/\gamma_0 = 0.16$. This condition is not met for solutions with pH 5 (the ratio is always less than 0.16) or for pH 7 and 7.5 (the ratio is always greater than 0.16); however, for pH 6.0 and 6.5 the ratio of the two moduli is in the region of 0.16 for much of the time while equilibrium is approached and is exactly this value after 6.2 and 3 h, respectively.

This maximum coupling enhances energy transfer between the two modes and aids the disaggregation of the micelles at the surface and prevents them reforming even after long aging times of the surface. The state of ionization of the copolymer molecules at these pH values is an attractive candidate as a source of this coupling but molecular theories are not available to be explored. In addition to resonance, another phenomenon that may occur in the surface modes is that of mode mixing, and this has been associated with the observation of negative dilational viscosities. To examine the possibility of this occurrence, the dispersion equation has been solved to provide capillary and dilational wave dampings and frequencies using typical values for γ_0 and ϵ_0 from Figure 5 for pH 6 and 6.5 and a range of ϵ' ; the results of these calculations are shown in Figure 8.

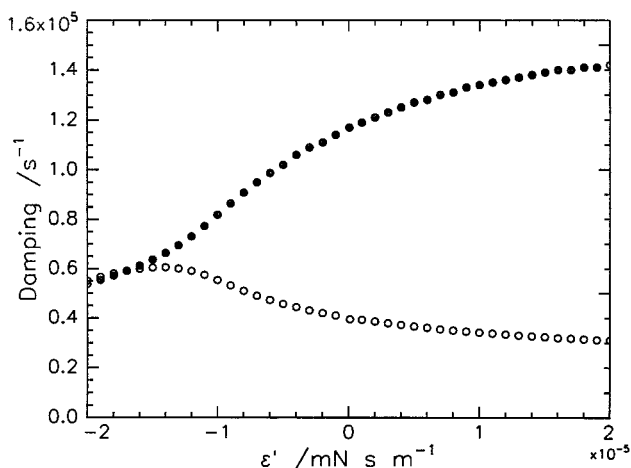


Figure 8. Calculated dilational (●) and capillary (○) mode damping as a function of dilational viscosity for $q = 1035 \text{ cm}^{-1}$, $\gamma_0 = 64 \text{ mN m}^{-1}$, and $\epsilon_0 = 11 \text{ mN m}^{-1}$.

When both dilational modulus and dilational viscosity are positive, the damping of the dilational mode increases. A negative dilational viscosity reduces the damping of the dilational mode, causing it to approach the damping of the capillary mode. Negative dilational viscosities have been observed in other polymer systems^{25–27} and in low molecular weight surfactant systems.²² They may be treated as an *effective* value symptomatic of the shortcomings in the dispersion equation.^{28,29} Phenomenologically, such negative values mean that the dilational mode has gained energy relative to that when $\epsilon' = 0$. The source of this energy is not defined, but in view of the resonance between the modes the capillary modes seem the most likely. In Figure 8 we note that the dilational mode damping does indeed approach the damping of the capillary mode, but mode mixing takes place at values of ϵ' far more negative than we observe here. What is perhaps more germane is the reduction in the *capillary* wave damping for positive dilational viscosities; i.e., the capillary mode becomes less stable. This instability may be a reflection of the disaggregation of the block copolymer micelles at the air–water interface in this pH range.

Conclusions

Surface quasi-elastic light scattering has been used to demonstrate that the equilibrium surface composition in solutions of a poly((dimethylamino)ethyl methacrylate–methyl methacrylate) block copolymer takes some hours to be established. For solutions of pH 6 and greater the absorption to the surface appears to be as micelles and remains as micelles for solutions of pH 7 and above. For pH 6 and 6.5 there is a slow disaggregation of the micelles, and the surface tension eventually rises to the high value of the pH 5 solution where the surface is populated by unimers. Despite the lower solubility of the copolymer at pH 6.5, the disaggregation process is faster at this pH than at pH 6.0. This has been attributed to the resonance between dilational and

capillary modes at pH 6.5, aiding the disaggregation by the ease of energy transfer between the two modes. Energy transfer takes place particularly to the dilational mode, leading to the observation of negative dilational viscosities.

Acknowledgment. We thank the EPSRC for funding the research program within the IRC of which this work has formed part.

References and Notes

- (1) Styrkas, D. A.; Butun, V.; Lu, J. R.; Keddie, J.; Armes, S. P. *Langmuir* **2000**, *16*, 5980–5986.
- (2) Langevin, D. *Light Scattering by Liquid Surfaces and Complementary Techniques*; Marcel Dekker: New York, 1992; Vol. 41.
- (3) Lucassen-Reynders, E. H.; Lucassen, J. *Adv. Colloid Interface Sci.* **1969**, *2*, 347–395.
- (4) Levich, V. G. *Physicochemical Hydrodynamics*; Prentice Hall: Englewood Cliffs, NJ, 1962.
- (5) Ingard, K. U. *Fundamentals of Waves and Oscillations*; Cambridge University Press: Cambridge, 1988.
- (6) Lucassen, J. *Trans. Faraday Soc.* **1968**, *64*, 2221–2229.
- (7) Goodrich, F. C. *J. Phys. Chem.* **1962**, *66*, 1858–1862.
- (8) Goodrich, F. C. *Proc. R. Soc. London A* **1981**, *374*, 341–370.
- (9) Buzza, D. M. A.; Jones, J. L.; McLeish, T. C. B.; Richards, R. W. *J. Chem. Phys.* **1998**, *109*, 5008–5024.
- (10) Baines, F. L.; Billingham, N. C.; Armes, S. P. *Macromolecules* **1996**, *29*, 3416–3420.
- (11) Earnshaw, J. C.; McGivern, R. C. *J. Colloid Interface Sci.* **1988**, *123*, 36–42.
- (12) Earnshaw, J. C. *J. Colloid Interface Sci.* **1990**, *138*, 282–283.
- (13) Earnshaw, J. C.; McGivern, R. C.; McLaughlin, A. C.; Winch, P. J. *Langmuir* **1990**, *6*, 649–660.
- (14) An, S. W.; Thomas, R. K.; Baines, F. L.; Billingham, N. C.; Armes, S. P.; Penfold, J. *J. Phys. Chem. B* **1998**, *102*, 5120–5126.
- (15) An, S. W.; Thomas, R. K.; Baines, F. L.; Billingham, N. C.; Armes, S. P.; Penfold, J. *J. Phys. Chem. B* **1998**, *102*, 387–393.
- (16) An, S. W.; Thomas, R. K.; Baines, F. L.; Billingham, N. C.; Armes, S. P.; Penfold, J. *Macromolecules* **1998**, *31*, 7877–7885.
- (17) Baines, F. L.; Armes, S. P.; Billingham, N. C.; Tuzar, Z. *Macromolecules* **1996**, *29*, 8151–8159.
- (18) Lee, A. S.; Gast, A. P.; Butun, V.; Armes, S. P. *Macromolecules* **1999**, *32*, 4302–4316.
- (19) Brandrup, J.; Immergut, E. H. *Polymer Handbook*; Wiley: New York, 1998.
- (20) Jones, R. A. L.; Richards, R. W. *Polymers at Surfaces and Interfaces*; Cambridge University Press: Cambridge, 1999.
- (21) Shusharina, N. P.; Linse, P.; Khokhlov, A. R. *Macromolecules* **2000**, *33*, 3892–3901.
- (22) Earnshaw, J. C.; McCoo, E. *Langmuir* **1995**, *11*, 1087–1100.
- (23) Pippard, A. B. *The Physics of Vibration*; Cambridge University Press: Cambridge, 1989.
- (24) Pippard, A. B. *Response and Stability*; Cambridge University Press: Cambridge, 1985.
- (25) Milling, A. J.; Richards, R. W.; Hiorns, R. C.; Jones, R. G. *Macromolecules* **2000**, *33*, 2651–2601.
- (26) Peace, S. K.; Richards, R. W.; Williams, N. *Langmuir* **1998**, *14*, 667–678.
- (27) Miller, A. F. Ph.D. Thesis, University of Durham, 2000.
- (28) Earnshaw, J. C.; McCoo, E. *Phys. Rev. Lett.* **1994**, *72*, 84–87.
- (29) Earnshaw, J. C.; McLaughlin, A. C. *Proc. R. Soc. London A* **1991**, *433*, 663–678.

MA001675P